

New Insights into the Role of Amines in the Synthesis of Molecular Sieves in Ionic Liquids

Renshun Xu, Weiping Zhang,* Jing Guan, Yunpeng Xu, Lei Wang, Huaijun Ma, Zhijian Tian, Xiuwen Han, Liwu Lin, and Xinhe Bao*^[a]

Abstract: A combination of state-of-the-art in situ one- and two-dimensional NMR spectroscopy and density functional theory (DFT) calculations have been employed for the first time to investigate the role of amines in the synthesis of aluminophosphate molecular sieves in ionic liquids (ILs). In situ rotating-frame nuclear Overhauser effect spectroscopy (ROESY) was used to demonstrate that the hybrid of imidazolium ionic liquids with organic amines, such as morpholine, connected through a hydrogen bond can be

formed in the gel during the crystallization of molecular sieves. By combining the characterizations of the final solid products obtained by using XRD analyses, solid-state NMR spectroscopy, thermogravimetric analysis, and DFT calculation results, it was verified that the hybrid between morpholine and

Keywords: density functional calculations · ionic liquids · molecular sieves · NMR spectroscopy · synthesis mechanisms

the imidazolium cation in the initial preparation stage can act as the structure-directing agent (SDA) for the synthesis of AFI-structured aluminophosphate molecular sieves. Our findings may suggest a synthesis mechanism of molecular sieves in ionic liquids in which the IL–organic amine hybrid is required in the nucleation step, whereas the crystal growth occurs through the occlusion of ionic liquids in the zeolite channels.

Introduction

The design and synthesis of inorganic porous materials with diverse compositions, structures, properties, and functions are important from both fundamental and technological points of view. Molecular sieves, especially aluminosilicate and aluminophosphate zeolites, are of interest in a number of areas such as catalysis and gas separation.^[1] In general, these materials can be made under hydrothermal or solvothermal conditions in which the organic amines are usually added as the templates or structure-directing agents (SDAs).^[2–7] The templating effect is thought to occur during either the gelation or nucleation process and involves the or-

ganic molecules organizing the inorganic tetrahedral units into a particular topology around themselves and thus providing the initial building block for further crystallization of a particular structure type.^[3] In some cases, two or more organic amines are needed in the synthesis of desired structures.^[8–12] The mixed organic molecules are often encapsulated inside the microporous network, and the nonbonded interactions between the organic amines and the microporous framework contribute to the stability of the system. These mixed organic amines can be regarded as cotemplates. Recently, a “cotemplating” strategy was applied to prepare some novel framework topologies.^[13] However, the nature of the templating effect during the crystallization of molecular sieves is not well understood because it is difficult to conduct an in situ spectroscopic study under the rigorous synthesis conditions, such as high pressure, of the hydrothermal or solvothermal processes.

In recent years, ionic liquids (ILs) have received much attention in many areas of chemistry and industry due to their potential as a “green” recyclable alternative to traditional organic solvents.^[14,15] The synthesis of inorganic porous solids in ILs is an emerging approach.^[16–18] A novel preparation method, termed ionothermal synthesis, was reported by Morris and Parnham using ILs or a eutectic mixture as both

[a] R. Xu, Prof. Dr. W. Zhang, J. Guan, Dr. Y. Xu, Dr. L. Wang, Dr. H. Ma, Prof. Dr. Z. Tian, Prof. X. Han, Prof. L. Lin, Prof. Dr. X. Bao
State Key Laboratory of Catalysis
Dalian Institute of Chemical Physics
Chinese Academy of Sciences
Dalian 116023 (China)
Fax: (+86) 411-8469-4447
E-mail: wpzhang@dicp.ac.cn
xhbao@dicp.ac.cn

Supporting information for this article is available on the WWW under <http://dx.doi.org/10.1002/chem.200802590>.

the solvent and template.^[18] Unlike conventional synthesis, ionothermal synthesis can be performed at ambient pressure due to the vanishingly low vapor pressure of almost all ILs, and is currently attracting great interest. To date, it has been used to prepare molecular sieves, zeolite analogues, inorganic–organic hybrids, and zeolite films, for example.^[19–29] Many of these structures are new, demonstrating the potential of this approach in the discovery of novel materials. Recently, a hydrogen-bond directing effect in the ionothermal synthesis of metal-coordinated polymers has been reported with the addition of organic amines.^[24] However, the role of organic amines was only studied in the final solid products. In our previous study, we found that the addition of organic amines into ILs can alter the crystallization process of aluminophosphate zeolites and result in better phase selectivity.^[25] This may provide opportunities for addressing fundamental questions like the role of amines in the zeolite synthesis by in situ spectroscopic investigations.

NMR spectroscopy is a unique tool that can probe the local structures and the molecular interactions of samples both in solution and in the solid state,^[30–32] and it is also a powerful analytical method for studying reaction processes in situ.^[33–35] Herein, we report the first application of in situ rotating-frame nuclear Overhauser effect spectroscopy (ROESY) in the investigation of the intermolecular interactions between the 1-butyl-3-methylimidazolium bromide ([bmim][Br]) IL and organic amines in the gel during the crystallization of aluminophosphate zeolites. By combining the characterizations of the final solid products obtained by solid-state magic-angle spinning (MAS) NMR spectroscopy and density functional theory (DFT) calculation results, the nature of the nonbonded interaction of the organic amines with cations of ILs has been revealed. This cooperative structure-directing effect in the initial crystallization stage results in the desired microporous structures in the final solids.

Results

In situ two-dimensional ROESY NMR spectra of the gel in the initial crystallization: To demonstrate the role of amines in the synthesis of molecular sieves, it is of interest to investigate the behavior of the gel precursors rather than to try to follow the crystal growth. In our study, morpholine (Morp) was added as an organic amine into the gel with ionic liquid [bmim][Br] (Figure 1) at 353 K. The imidazoli-

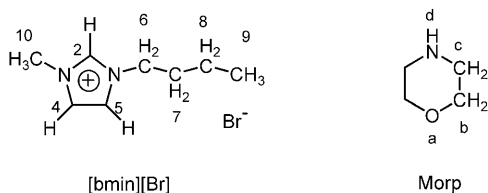


Figure 1. Chemical structures and atom numbering for [bmim][Br] and Morp.

um cation–cation interaction and cation–organic amine interaction were studied by means of the homonuclear Overhauser effect (NOE) in the rotating frame. The in situ ^1H – ^1H ROESY spectrum in Figure 2 shows significant intermolecu-

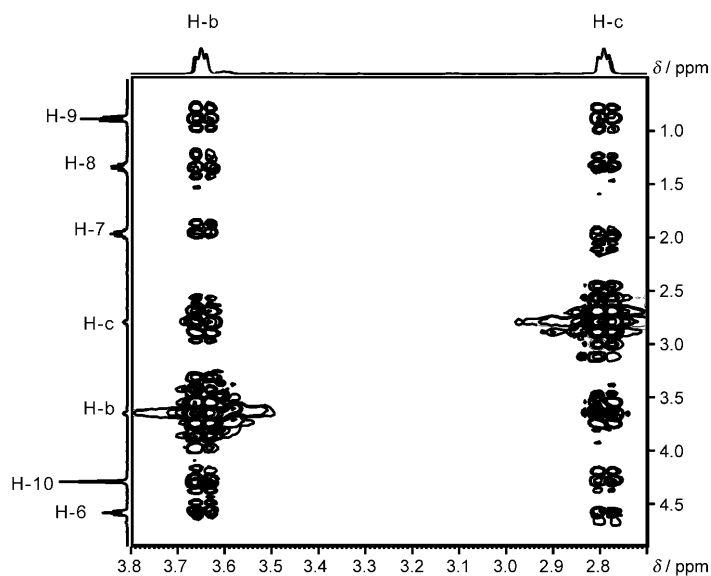


Figure 2. In situ ^1H – ^1H NMR ROESY spectra of the [bmim][Br] and organic amine mixture with a molar composition of [bmim][Br]/Morp (40:2–5). The spectrum was acquired at 353 K with a mixing time of 600 ms.

lar cross peaks of Morp protons (H-b and H-c) with imidazolium protons (H-6, H-7, H-8, H-9, and H-10). The presence of cross peaks indicates the intermolecular distance between [bmim][Br] and Morp is less than 4 Å in terms of the NOE principles.^[36] For the IL system, the presence of cross peaks in the ROESY spectra means an intermolecular hydrogen bond formed.^[31] As a potential electron-pair donor, amine can form hydrogen bonds with the imidazolium ring of ILs.^[24] In our case, a specific hydrogen atom (H-2) of the imidazolium cation can be shared by the oxygen or nitrogen atom of Morp through a hydrogen bond because imidazolium ionic liquids are polymeric supramolecules, in which the strongest hydrogen bond involves the most acidic proton (H-2) of the imidazolium cation.^[37] Therefore, a hybrid structure of the [bmim]⁺ cation with organic amine molecules through intermolecular hydrogen-bond interactions was formed in the ILs. In addition, the appearance of the cross peaks of the imidazolium cation–cation protons also indicates that the addition of organic amines cannot fully disrupt the intermolecular interactions between imidazolium cations. When adding H_3PO_4 acid into the above system at 353 K, the intermolecular interactions of ILs with organic amines can still be observed (see Figure S1 in the Supporting Information). By increasing the temperature to 413 K, the intermolecular cross peaks of imidazolium protons with Morp disappear (see Figure S1 in the Supporting Information). So, it seems that there are strong interactions of H_3PO_4 with the organic amines at higher temperature. The

absence of cross peaks may be due to the charge repulsions between protonated amines and the imidazolium cation at higher temperature. By further adding aluminum isopropoxide into the above-mentioned system at 413 K for crystallization, the in situ ^1H - ^1H ROESY spectrum in Figure 3 shows again the intermolecular cross peaks of Morp protons (H-b and H-c) with imidazolium protons (H-6, H-7, H-8, H-9, and H-10). So, it seems that the hybrid structures of ILs with organic amines recover again during the crystallization process. This may be due to the rapid condensation of H_3PO_4 with $\text{Al}[\text{OCH}(\text{CH}_3)_2]_3$ at the crystallization temperature to form the Al-O-P species, which releases the organic amines to again form the hydrogen-bonded structures with ILs.

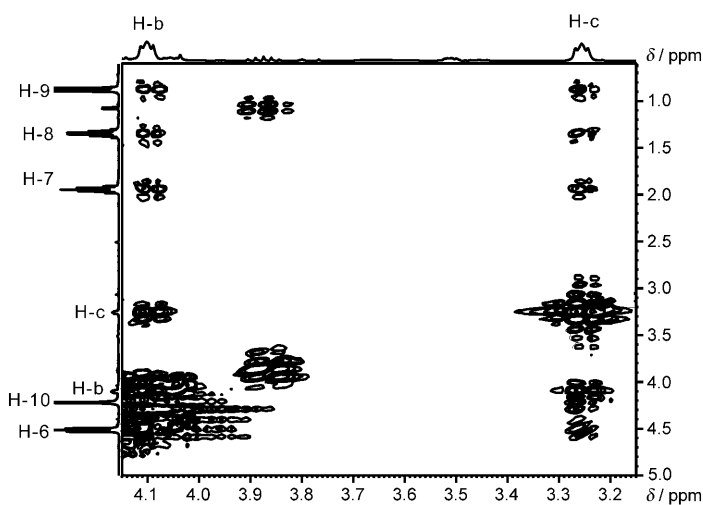


Figure 3. In situ ^1H - ^1H NMR ROESY spectra of the synthesis gel with a molar composition of $\text{Al}_2\text{O}_3/\text{P}_2\text{O}_5/\text{HF}/[\text{bmim}][\text{Br}]/\text{Morp}$ (1:3:0.4:40:2-5). The spectrum was acquired at 413 K with a mixing time of 600 ms.

Characterization of the solid products at different crystallization stages: Figure 4 shows the XRD patterns of the samples synthesized at different crystallization stages. It was found that only the amorphous phase was obtained with a crystallization time of up to 3 h at 413 K. Increasing the crystallization time to 4 h results in the appearance of reflections identical to AFI-structured zeolites but with less crystallinity. Further heating of the gel for 12 h leads to completely crystalline $\text{AlPO}_4\text{-5}$ with AFI structures. The local structures of the resultant samples were also investigated by one- and two-dimensional solid-state MAS NMR spectroscopy (see Figures S2 and S3 in the Supporting Information). It was found that the intensity of tetrahedral Al increased followed by the decrease of the octahedral Al, and the intensity of fully condensed P increased followed by the decrease of partially condensed P as the crystallization time increased. As for the 12 h sample, nearly all the Al and P atoms sit in the zeolitic framework as AlO_4 and PO_4 tetrahedrons, and are connected through the Al-O-P bonds as indicated by the 2D ^{27}Al , ^{31}P heteronuclear correlation (HETCOR) spectra.

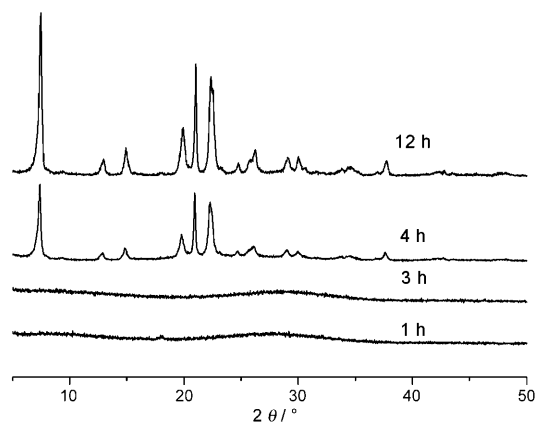


Figure 4. XRD patterns of samples synthesized from a gel with a molar composition of $\text{Al}_2\text{O}_3/\text{P}_2\text{O}_5/\text{HF}/[\text{bmim}][\text{Br}]/\text{amine}$ (1:3:0.4:40:2-5) after different crystallization times at 413 K.

The state of the structure-directing agent inside the AFI channels can be followed by thermogravimetric analysis and ^{13}C NMR spectroscopy. Figure 5 shows the differential

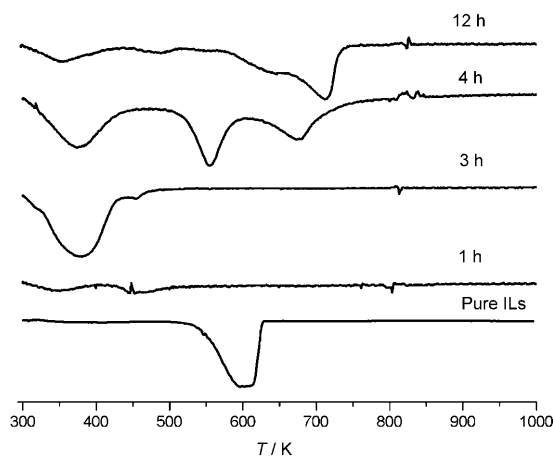


Figure 5. DTG curves of bulk $[\text{bmim}][\text{Br}]$ and the solid products with different crystallization times.

thermogravimetric (DTG) curves of the as-synthesized samples. Before taking the measurements, all the samples were washed thoroughly with deionized water to remove the remaining ILs on the external surfaces. It can be seen that the maximum decomposition temperature of the 1 and 3 h samples is below 450 K; this weight loss may be due to the desorption of water, and neither Morp nor IL weight loss can be observed. As for the 4 h sample, two weight-loss peaks can be observed between 500 and 800 K. The weight loss at 670 K could be due to the decomposition of the ILs inside $\text{AlPO}_4\text{-5}$ zeolites, whereas the weight loss at 550 K may be ascribed to the decomposition of Morp. For the 12 h sample, the maximum decomposition temperature of the ILs shifts to 700 K, and the weight-loss peak of Morp becomes weaker than in the 4 h sample. It can be seen that the maximum decomposition temperature of the ILs in solid products is be-

tween 670 and 700 K, which is higher than that of the bulk ILs (≈ 600 K). This may be due to the occlusion of $[\text{bmim}]^+$ inside the zeolite channels. So, the DTG analysis indicates that both ILs and Morp are included in the AFI channels, and furthermore, that the weight ratio of Morp to ILs decreases with increasing crystallization time. Figure 6 shows

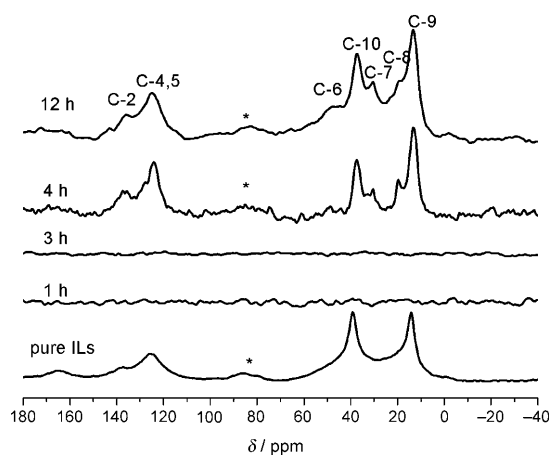


Figure 6. $^1\text{H} \rightarrow ^{13}\text{C}$ CP/MAS NMR spectra of $[\text{bmim}][\text{Br}]$ crystals and the solid samples with different crystallization times at 413 K. Each spectrum was acquired with a contact time of 6 ms and a 4 s recycle delay. * indicates the spinning sidebands.

the room-temperature $^1\text{H} \rightarrow ^{13}\text{C}$ CP/MAS NMR spectra of $[\text{bmim}][\text{Br}]$ IL crystals and solid products with different crystallization time in the presence of $[\text{bmim}][\text{Br}]$ and morpholine. Neither the IL cation nor Morp signals can be observed for the 1 and 3 h samples. As for the 4 and 12 h samples, each spectrum has almost the same feature, that is, there is no new signal except for $[\text{bmim}]^+$. However, the signals of $[\text{bmim}]^+$ in the $\text{AlPO}_4\text{-5}$ zeolites shift upfield and are better resolved relative to the bulk counterparts. This demonstrates that $[\text{bmim}]^+$ cations are occluded in the pore spaces of $\text{AlPO}_4\text{-5}$ zeolites, which results in the breakage of the hydrogen bonds between $[\text{bmim}]^+$ cations in bulk crystals and in a decrease of the dipole-dipole interactions between them. It should be noted that there are no signals of morpholine in the ^{13}C solid-state NMR spectra although the addition of organic amines to ILs can facilitate the formation of $\text{AlPO}_4\text{-5}$. This may be due to the low content of organic amines in the synthesis gel; their signals are buried in the broad lines of the ILs. To verify the occlusion of organic amines in $\text{AlPO}_4\text{-5}$, the resultant solid samples were dissolved with concentrated HCl solution, and characterized by means of solution ^{13}C NMR spectroscopic techniques (Figure 7). Similarly, neither a Morp nor imidazolium cation signal is observed for the 1 and 3 h samples. With increasing crystallization time, both the signals of organic amines and IL cations can be observed, and the relative content of morpholine to imidazolium decreases clearly. So, the DTG analysis, and solid-state and solution ^{13}C NMR spectroscopy results indicate that large $[\text{bmim}]^+$ cations with minor organic

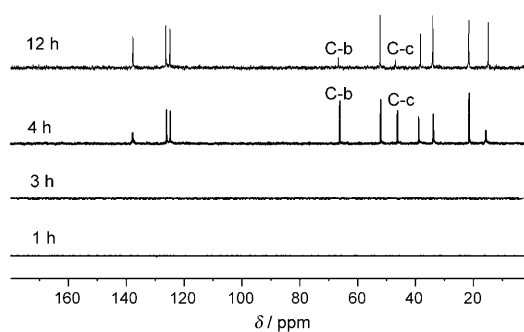


Figure 7. Solution ^{13}C NMR spectra of the solid samples dissolved in HCl, which were synthesized with $[\text{bmim}][\text{Br}]$ and Morp with different crystallization times at 413 K.

amines are occluded in the channels of $\text{AlPO}_4\text{-5}$ zeolites with increasing crystallization time.

DFT calculations: Experimental studies on the location and conformation adopted by the template molecules inside the zeolitic hosts are not so straightforward using solid-state NMR spectra because of the broad-spectrum feature caused by the strong dipolar interaction, for example. Theoretical computations in recent years have made rapid progress in the accurate calculation of molecular structures, energetics, dynamics, and so forth, which provide deeper understanding of the synthesis processes.^[5,38–39] To further evaluate the role of the hybrid formed by the $[\text{bmim}]^+$ cation and Morp in the stabilization of the AFI structure, we optimized the geometries of $[\text{bmim}]^+$ -Morp, the AFI framework, and the AFI- $[\text{bmim}]^+$ -Morp adsorption complex, respectively (Figure 8; Figure S4 in the Supporting Information). The final stabilization energy (E_{stab}) can be represented by the difference of the energies according to Equation (1):

$$\Delta E_{\text{stab}} = E_{\text{AFI-}[\text{bmim}]^+\text{-Morp}} - E_{\text{AFI}} - E_{[\text{bmim}]^+\text{-Morp}} \quad (1)$$

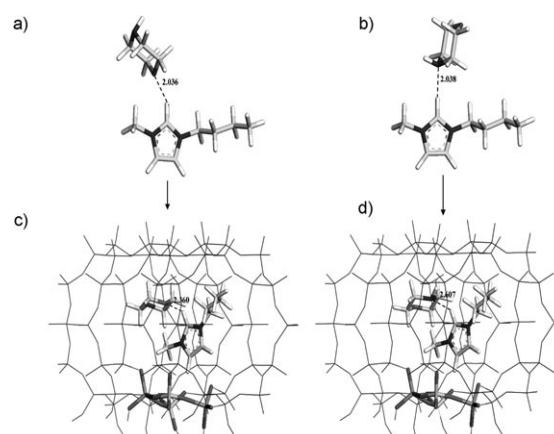


Figure 8. Optimized structures of the hybrids of the $[\text{bmim}]^+$ cation with Morp: a) $[\text{bmim}]^+$ -Morp-O, b) $[\text{bmim}]^+$ -Morp-N; and the hybrids occluded in the $\text{AlPO}_4\text{-5}$ zeolites with AFI structure: c) AFI- $[\text{bmim}]^+$ -Morp-O, d) AFI- $[\text{bmim}]^+$ -Morp-N.

As can be seen from Figure 8, the hybrid structures of [bmim]⁺-Morp are characterized by the strong hydrogen bonds formed between the acidic proton H-2 (connected to the carbon atom that is located between the N atoms) in the [bmim]⁺ cation and the N or O atom in Morp, with hydrogen-bond lengths of 2.036 (O donor) and 2.038 Å (N donor), respectively. In the adsorption complex of AFI-[bmim]⁺-Morp, the hybrid structures of [bmim]⁺-Morp can be intercalated into the 12-membered ring of an AFI channel, in which the hydrogen bonds present in the original hybrid structures of [bmim]⁺-Morp could be retained. However, the distances between the acidic proton (H-2) of [bmim]⁺ and the O or N atom of Morp are increased to 2.360 Å for the former and 2.607 Å for the latter. In addition, weak interactions are found between the terminal CH₂ fragment in the 5-membered ring of [bmim]⁺ and the nearest framework oxygen atoms. Our results show that ΔE_{stab} values for the AFI-[bmim]⁺-Morp system are -69.2 (O donor) and -57.3 kcal mol⁻¹ (N donor), respectively. This means that the formation of the AFI structure, that is, AlPO₄-5 zeolites, is favorable with the insertion of [bmim]⁺-Morp, verifying that the hybrid between the imidazolium cation and organic amine formed in the gel stage could be acting as a structure-directing agent for the synthesis of AFI-structured molecular sieves.

Discussion

From the above-mentioned results it is clear that in the ionothermal synthesis of aluminophosphate molecular sieves, the pure AFI structure can be obtained in the presence of morpholine and [bmim][Br]. The [bmim][Br] ILs alone are not the SDAs for the AFI structure;^[25] therefore, we speculate that morpholine may exert a structure-directing effect together with ionic liquids. The intermolecular interactions of ILs with Morp can be observed by in situ ROESY NMR spectroscopic techniques during the crystallization process. As shown in Figure 3, we do see the dipole-dipole interaction between the imidazolium cation and Morp in the gel, which means a hybrid of the imidazolium cation with Morp is formed through the hydrogen bond during the crystallization process. This hybrid may act as the cooperative structure-directing agent for the synthesis of the AFI structure. The crystallization process of AlPO₄-5 was studied in detail by using DTG analyses and NMR spectroscopy. For the solid sample at a short crystallization time (ca. 4 h), which is also dissolved in a concentrated HCl solution, the ¹³C NMR spectrum and DTG curves show that both morpholine and imidazolium can be observed. However, for the well-crystallized solid products, NMR spectra and DTG results indicate that there are minor Morp and large imidazolium cations in the AFI channels. These may suggest a possible mechanism for the synthesis of the AFI structure in ILs in which a small amount of the hybrid of imidazolium with morpholine as a SDA provides the initial nucleation selectivity, then large imidazolium cations act as the pore-fill-

ing agents for the crystal growth. The DFT calculation results also provide evidence for intermolecular interactions between imidazolium cations and morpholine either in the IL system or in the AFI channels, further supporting the cooperative structure-directing effect of the IL-organic amine hybrid. Our findings are in accord with the recent work of Gómez-Hortigüela et al.^[39] for the synthesis of the AFI structure in supramolecular solution in which minor benzylpyrrolidine molecules are required for the formation of the initial nuclei, then the crystal growth process can occur through occlusion of single molecular SDA units. Zones et al.^[10-12] also proposed a new zeolite synthesis system in which a minor SDA is used to selectively specify the nucleation product, then a larger amount of other amines is used to provide pore-filling agents for the crystal growth. So, our work further provides evidence for the importance of SDAs in the nucleation with regard to the phase selectivity. Once nucleation has been initiated by the imidazolium-organic amine hybrid, a large number of imidazolium cations can be filled in the AFI phase and thus promote further crystal growth.

Conclusion

In summary, the role of organic amines in the ionothermal synthesis has been studied in detail by using both state-of-the-art in situ NMR spectroscopy and density functional theoretical studies. It is verified that a hybrid of morpholine with a imidazolium cation can be formed through a hydrogen bond during the crystallization of aluminophosphate molecular sieves. This hybrid that is formed in the gel stage could act as a cooperative structure-directing agent for the specific AFI structure in the final solids. Our results may suggest a synthesis mechanism of molecular sieves in ionic liquids in which the IL-organic amine hybrid is required in the nucleation step, whereas the crystal growth occurs through the occlusion of ionic liquids. These findings may offer new insight into the ionothermal or even hydrothermal synthesis of molecular sieves. It seems that even a weak nonbonded interaction in the template molecules, such as the organic amines with ILs in the gel, can drastically alter the structure-directing property.

Experimental Section

Sample preparation: The ionothermal synthesis of molecular sieves in ionic liquids was carried out according to our previously reported procedures.^[25,26] In general, a round-bottomed flask was charged with [bmim][Br] (23 g), H₃PO₄ (1.80 g, 85 wt % in water), Al[OCH(CH₃)₂]₃ (1.06 g), and HF (0.05 g, 40 wt % in water). Amine was added if required. The crystallization temperature was 413 K in an oil bath for as long as 1–12 h. After cooling to room temperature, the products were washed with distilled water and ethanol, and dried at 393 K overnight. All samples were characterized by powder X-ray diffraction on a Rigaku D/Max-2500 diffractometer using Cu_{K α} radiation.

Solution and solid-state NMR spectroscopy measurements: All the solution NMR spectroscopy experiments were performed on a Bruker DRX-400 spectrometer using a D₂O or DMSO capillary for the lock. ¹H and ¹³C NMR spectra were acquired at 400.13 and 100.62 MHz, respectively. Their chemical shifts were referenced to tetramethylsilane (TMS). AlPO₄-5 zeolites with templates were dissolved in a concentrated HCl solution. The solution was collected, and analyzed by solution ¹³C NMR spectroscopy. Two-dimensional ROESY experiments were performed in situ at desired temperatures in the time proportional phase incrementation (TPPI) phase-sensitive mode with a recycle delay of 1 s, a mixing time of 600 ms, 256 increments in the *f*₁ field, and 64 scans per increment.

All the solid-state NMR spectroscopy measurements were performed on a Varian Infinityplus-400 spectrometer equipped with 2.5, 4.0, and 7.5 mm MAS probes. ¹H → ¹³C CP/MAS NMR spectra were recorded at 100.5 MHz with a spinning rate of 4 kHz, 2100 scans, a contact time of 2.5 ms, and a recycle delay of 2 s. ²⁷Al MAS NMR spectra were recorded at 104.2 MHz with a spinning rate of 10 kHz, 200 scans, and a 2 s recycle delay. The chemical shifts were referenced to a 1% Al(NO₃)₃ aqueous solution. ³¹P MAS NMR spectroscopy experiments with high-power proton decoupling were conducted at 161.8 MHz with a spinning rate of 10 kHz, 200 scans, and a 4 s recycle delay. The chemical shifts were referenced to 85% H₃PO₄. The two-dimensional ²⁷Al triple-quantum (3Q) MAS NMR experiments were performed by using a three-pulse sequence incorporating a *z* filter at a spinning speed of 25 kHz with the 2.5 mm probe.^[40] The two-dimensional ²⁷Al–³¹P HETCOR spectra were acquired by using the approach described by Fyfe et al.^[41] The TPPI method was used in the 2D data acquisition and processing.

Theoretical calculation details: To theoretically investigate the guest–host interaction, the structure of the 60T cluster, including 226 atoms of the straight channel in which the adsorbates can be trapped, was taken from the lattice structure of AFI zeolite. Hydrogen atoms were used to saturate the extraneous bonds at the edge of the cluster and the orientation of H was along the pre-existing lattice. The structures of the hybrid [bmim]⁺–Morp were first obtained with the acidic proton (connected to the carbon atom that is located between the N atoms) in the [bmim]⁺ cation directing towards the N or O atom in Morp. Then in the adsorption system, the [bmim]⁺–Morp complex was put inside the cavity of AFI to study the role of this hybrid in the stabilization of the AFI structure in the final solids. The ONIOM2 scheme^[42] in which the whole model is subdivided into two layers was adopted for computational efficiency. The high inner layer representing the active region and consisting of the adsorbate molecules and the 4T cluster (atoms drawn as sticks in Figure 8) was treated with the B3LYP/6-31G(d,p) method. The rest of the extended framework environment was treated by using less-expensive levels of theory, namely, the molecular mechanics force field (UFF) to reduce the required computational time and to practically represent the confinement effect of the zeolite pore structure, which is mainly due to van der Waals interactions. This ONIOM2 method has been proven to be an accurate and practical model for exploring the structure, adsorption properties, and reaction mechanisms taking place inside zeolite pores.^[43–45] All our calculations were performed by using the Gaussian 03 program.^[46] To avoid losing the unique structure of the zeolites during structure optimization, only the active site region and the adsorbates were allowed to relax, and the remaining atoms of the cluster model were fixed at their crystallographic locations.

Acknowledgements

We are grateful for the financial support of the National Natural Science Foundation of China (no. 20873140) and Ministry of Science and Technology of China through the National Key Project of Fundamental Research (no. 2009CB623507). We thank the anonymous reviewers for fruitful discussions and suggestions.

- [1] C. S. Cundy, P. A. Cox, *Chem. Rev.* **2003**, *103*, 663.
- [2] B. M. Lok, T. R. Cannan, C. A. Messina, *Zeolites* **1983**, *3*, 282.
- [3] S. L. Burkett, M. E. Davis, *J. Phys. Chem.* **1994**, *98*, 4647.
- [4] C. S. Cundy, P. A. Cox, *Microporous Mesoporous Mater.* **2005**, *82*, 1.
- [5] G. Sastre, A. Cantin, M. J. Díaz-Cabañas, A. Corma, *Chem. Mater.* **2005**, *17*, 545.
- [6] A. Corma, F. Rey, J. Rius, M. J. Sabater, S. Valencia, *Nature* **2004**, *431*, 287.
- [7] J. H. Yu, R. R. Xu, *Chem. Soc. Rev.* **2006**, *35*, 593.
- [8] A. Kuperman, S. Nadimi, S. Oliver, G. A. Ozin, J. M. Garces, M. M. Olken, *Nature* **1993**, *365*, 239.
- [9] S. J. Weigel, S. C. Weston, A. K. Cheetham, G. D. Stucky, *Chem. Mater.* **1997**, *9*, 1293.
- [10] S. I. Zones, Y. Nakagawa, L. T. Yuen, T. V. Harris, *J. Am. Chem. Soc.* **1996**, *118*, 7558.
- [11] S. I. Zones, S. J. Hwang, M. E. Davis, *Chem. Eur. J.* **2001**, *7*, 1990.
- [12] S. I. Zones, S. J. Hwang, *Chem. Mater.* **2002**, *14*, 313.
- [13] M. Castro, R. Garcia, S. J. Warrender, A. M. Z. Slawin, P. A. Wright, P. A. Cox, A. Fecant, C. Mellot-Draznieks, N. Bats, *Chem. Commun.* **2007**, 3470.
- [14] T. Welton, *Chem. Rev.* **1999**, *99*, 2071.
- [15] R. D. Rogers, K. R. Seddon, *Science* **2003**, *302*, 792.
- [16] M. Antonietti, D. Kuang, B. Smarsly, Y. Zhou, *Angew. Chem.* **2004**, *116*, 5096; *Angew. Chem. Int. Ed.* **2004**, *43*, 4988.
- [17] A. Taubert, Z. H. Li, *J. Chem. Soc. Dalton Trans.* **2007**, 723.
- [18] E. R. Parnham, R. E. Morris, *Acc. Chem. Res.* **2007**, *40*, 1005.
- [19] E. R. Cooper, C. D. Andrews, P. S. Wheatley, P. B. Webb, P. Wormald, R. E. Morris, *Nature* **2004**, *430*, 1012.
- [20] E. R. Parnham, R. E. Morris, *J. Am. Chem. Soc.* **2006**, *128*, 2204.
- [21] E. R. Parnham, E. A. Drylie, P. S. Wheatley, A. M. Z. Slawin, R. E. Morris, *Angew. Chem.* **2006**, *118*, 5084; *Angew. Chem. Int. Ed.* **2006**, *45*, 4962.
- [22] E. R. Parnham, R. E. Morris, *Chem. Mater.* **2006**, *18*, 4882.
- [23] E. A. Drylie, D. S. Wragg, E. R. Parnham, P. S. Wheatley, A. M. Z. Slawin, J. E. Warren, R. E. Morris, *Angew. Chem.* **2007**, *119*, 7985; *Angew. Chem. Int. Ed.* **2007**, *46*, 7839.
- [24] Z. J. Lin, Y. Li, A. M. Z. Slawin, R. E. Morris, *Dalton Trans.* **2008**, 3989.
- [25] L. Wang, Y. P. Xu, Y. Wei, J. C. Duan, A. B. Chen, B. C. Wang, H. J. Ma, Z. J. Tian, L. W. Lin, *J. Am. Chem. Soc.* **2006**, *128*, 7432.
- [26] Y. P. Xu, Z. J. Tian, S. J. Wang, Y. Hu, L. Wang, B. C. Wang, Y. C. Ma, L. Hou, J. Y. Yu, L. W. Lin, *Angew. Chem.* **2006**, *118*, 4069; *Angew. Chem. Int. Ed.* **2006**, *45*, 3965.
- [27] H. J. Ma, Z. J. Tian, R. S. Xu, B. C. Wang, Y. Wei, L. Wang, Y. P. Xu, W. P. Zhang, L. W. Lin, *J. Am. Chem. Soc.* **2008**, *130*, 8120.
- [28] H. Z. Xing, J. Y. Li, W. F. Yan, P. Cheng, Z. Jin, J. H. Yu, S. Dai, R. R. Xu, *Chem. Mater.* **2008**, *20*, 4179.
- [29] R. Cai, M. W. Sun, Z. W. Chen, R. Munoz, C. O'Neill, D. E. Beving, Y. S. Yan, *Angew. Chem.* **2008**, *120*, 535; *Angew. Chem. Int. Ed.* **2008**, *47*, 525.
- [30] G. Engelhardt, D. Michel, *High-Resolution Solid-state NMR of Silicates and Zeolites*, Wiley, New York, **1987**.
- [31] A. Mele, C. D. Tran, S. H. D. P. Lacerda, *Angew. Chem.* **2003**, *115*, 4500; *Angew. Chem. Int. Ed.* **2003**, *42*, 4364.
- [32] J. D. Epping, B. F. Chmelka, *Curr. Opin. Colloid Interface Sci.* **2006**, *11*, 81.
- [33] J. F. Haw, P. W. Goguen, T. Xu, T. W. Skloss, W. G. Song, Z. K. Wang, *Angew. Chem.* **1998**, *110*, 993; *Angew. Chem. Int. Ed.* **1998**, *37*, 948.
- [34] X. W. Han, Z. M. Yan, W. P. Zhang, X. H. Bao, *Curr. Org. Chem.* **2001**, *5*, 1017.
- [35] M. Hunger, J. Weitkamp, *Angew. Chem.* **2001**, *113*, 3040; *Angew. Chem. Int. Ed.* **2001**, *40*, 2954.
- [36] R. A. Mantz, P. C. Trulove, R. T. Carlin, R. A. Osteryoung, *Inorg. Chem.* **1995**, *34*, 3846.
- [37] J. Dupont, *J. Braz. Chem. Soc.* **2004**, *15*, 341.
- [38] G. Yang, X. C. Liu, X. W. Han, X. H. Bao, *J. Phys. Chem. B* **2006**, *110*, 23388.

- [39] L. Gómez-Hortigüela, F. López-Arbeloa, F. Corà, J. Pérez-Pariente, *J. Am. Chem. Soc.* **2008**, *130*, 13274.
- [40] X. J. Li, W. P. Zhang, S. L. Liu, L. Y. Xu, X. W. Han, X. H. Bao, *J. Phys. Chem. C* **2008**, *112*, 5955.
- [41] C. A. Fyfe, K. T. Mueller, H. Grondy, K. C. Wong-Moon, *J. Phys. Chem.* **1993**, *97*, 13484.
- [42] F. Maseras, K. Morokuma, *J. Comput. Chem.* **1995**, *16*, 1170.
- [43] S. Kasuriya, S. Namuangruk, P. Treesukol, M. Tirtowidjojo, J. Limtrakul, *J. Catal.* **2003**, *219*, 320.
- [44] K. Bobuatong, J. Limtrakul, *Appl. Catal. A* **2003**, *253*, 49.
- [45] B. Jansang, T. Nanok, J. Limtrakul, *J. Phys. Chem. C* **2008**, *112*, 540.
- [46] Gaussian 03, Revision B.05, M. J. Frisch, G. W. Trucks, H. B. Schlegel, G. E. Scuseria, M. A. Robb, J. R. Cheeseman, J. A. Montgomery, Jr., T. Vreven, K. N. Kudin, J. C. Burant, J. M. Millam, S. S. Iyengar, J. Tomasi, V. Barone, B. Mennucci, M. Cossi, G. Scalmani, N. Rega, G. A. Petersson, H. Nakatsuji, M. Hada, M. Ehara, K. Toyota, R. Fukuda, J. Hasegawa, M. Ishida, T. Nakajima, Y. Honda, O. Kitao, H. Nakai, M. Klene, X. Li, J. E. Knox, H. P. Hratchian, J. B. Cross, C. Adamo, J. Jaramillo, R. Gomperts, R. E. Stratmann, O. Yazyev, A. J. Austin, R. Cammi, C. Pomelli, J. W. Ochterski, P. Y. Ayala, K. Morokuma, G. A. Voth, P. Salvador, J. J. Dannenberg, V. G. Zakrzewski, S. Dapprich, A. D. Daniels, M. C. Strain, O. Farkas, D. K. Malick, A. D. Rabuck, K. Raghavachari, J. B. Foresman, J. V. Ortiz, Q. Cui, A. G. Baboul, S. Clifford, J. Cioslowski, B. B. Stefanov, G. Liu, A. Liashenko, P. Piskorz, I. Komaromi, R. L. Martin, D. J. Fox, T. Keith, M. A. Al-Laham, C. Y. Peng, A. Nanayakkara, M. Challacombe, P. M. W. Gill, B. Johnson, W. Chen, M. W. Wong, C. Gonzalez, J. A. Pople, Gaussian, Inc., Pittsburgh, PA, **2003**.

Received: December 10, 2008
Published online: March 26, 2009